CHAPTER 87

ONSHORE-OFFSHORE SEDIMENT MOVEMENT ON A BEACH

P. Nielsen[1] I. A. Svendsen[2] C. Staub[3]

ABSTRACT

A theoretical model is developed for the movement of loose sediments in oscillatory flow with or without a net current. In the present formulation the model is two-dimensional, but may readily be extended to three dimensions.

It is assumed that all movement of sediments occurs in suspension, and exact analytical solutions are given for the time variation of the concentration profile, the instantaneous sediment flux and the net flux of sediment over a wave period. The model requires as empirical input a diffusion coefficient ε and pick-up function p(t), for which experimental data are presented. Two examples are discussed in detail, illustrating important aspects of the onshore-offshore sediment motion.

1. INTRODUCTION

The motion of loose sediments perpendicular to the coastline is one of many unsolved problems in sediment transport due to waves and currents. Yet it is generally agreed that this particular phenomenon plays a vital part in the sorting of sediments on a coast and hence has important bearing on the question of which grain sizes are present in the surf zone, where the bulk of the longshore transport takes place.

In nature the lateral sediment transport depends strongly on three-dimensional effects which are responsible for the often significant net water motions that occur in particular in the surf zone. Here the net water flux is shorewards in areas where the bottom configuration creates heavy breaking, and seawards (sometimes as rip-currents) in the often deeper areas where the breaking is weak or absent, moving as a longshore current between these regions. Also appreciable time variations occur over some minutes and may even dominate the spatial variations.

Though obviously crucial for the net movement of sediments it is beyond the scope of the present paper to analyse this water motion further. In the following we shall assume that the water motion is known. This is further justified by the observation that the processes involved in the local movement of sediments, which we are going to analyse, are almost exclusively governed by the local flow conditions. The purpose of the present paper is to formulate a theory that as closely as possible models the important part of the processes which can be observed to occur in sediment motion under waves.

---

[1]Ph.D.-student, [2]Assoc. Professor, [3]Graduate student
Institute of Hydrodynamics and Hydraulic Engineering (ISVA),
Technical University of Denmark, Building 115, DK-2800 Lyngby.

2. PHYSICAL DESCRIPTION

To do so it is important first to describe the nature of the phenomenon.

Bottom configuration

One of the basic aspects is the bottom configuration generated by the water motion. It is well known that for a wide range of wave and sand parameters ripples are formed on the bed. The size, steepness and shapes of these have been measured by numerous authors (see e.g. Inman (1957) and Dingler (1974)), and lately Nielsen (1977) showed that the steepness of the ripples (measured ratio between height η from trough to crest over distance λ between two successive crests) is almost constant (0.15 to 0.20) for a value of the Shields' parameter θ' less than about 0.4, where θ' is defined as

$$\theta' \equiv \frac{1}{2} a^2 \omega^2 f_w/(s-1)\, g\, d) \tag{1}$$

with a the amplitude of water particle motion at the bottom, $\omega = 2\pi/T$, T being the wave period. f_w is a friction factor, s and d are specific gravity and mean diameter, respectively, of the sand grains. g is the acceleration of gravity.

For θ' increasingly larger than 0.4 the steepnes of the ripples decreases rapidly, and for $\theta' > 1$ the bed is virtually plane with relatively gentle undulations.

These are general trends subject to considerable scattering in the individual cases, in particular when field conditions in irregular waves are considered. Nevertheless it shows that except for very high storm waves, the sand on natural beaches (most often having $d \approx 0.2 - 0.3$ mm) will yield θ'-values not larger than 1. (A wave height $H = 10$ m, say, on a water depth $h = 15$ m yields $\theta' \sim 5$), which again implies that most often the bed will be covered by ripples.

Since it turns out that the ideas presented later in this paper can readily be adopted to a plane bottom, we first focus on the flow over a ripple bed.

Oscillatory flow over a ripple bed

The ripples formed by the oscillatory particle motion under waves are entirely different from the bed forms known from steady flow (see e.g. Allen (1968)). Also the oscillatory flow itself and the mechanisms by which the sediment is moved show little resemblance with unidirectional flow patterns.

This is due to the strong pressure gradients associated with the oscillatory flow which create strong lee eddies during the phase where the main flow is retarded, i.e. twice every wave period. Successively at the turn of the flow these eddies are 'washed' out into the main flow, thus yielding dominant contribution to the general turbulence level, and carrying appreciable amounts of sediment out in suspension (Fig. 1). Excellent photos showing details of the development of the eddy and a description of the process were presented by Bijker et al. (1976). Also Nakoto et al. (1977) describe the sequence.

One of the important features is the large velocities in the lee eddy. In fact the adverse velocity is of the same magnitude as the

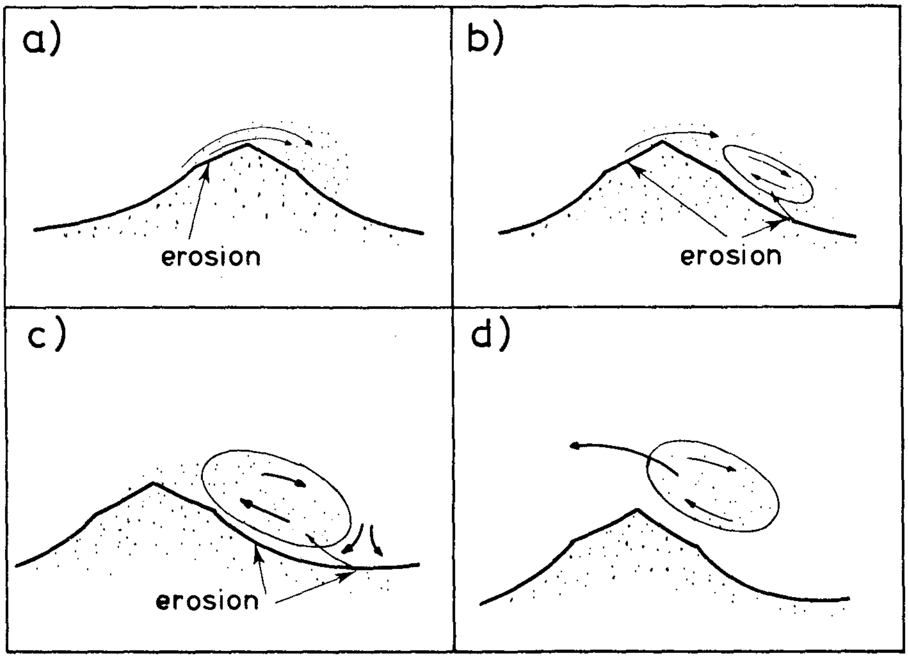

Fig. 1 Pick-up mechanism over a rippled bed. a) Velocity increasing, no separation, no effective pick-up. b) Velocity decreasing, separation started, sand accumulation in vortex. c) Water velocity vanishing, the vortex is fully developed. d) Water velocity reverses, the vortex is lifted out. This is when the effective pick-up takes place.

velocity in the main flow outside (Tunsdall and Inman (1975)), in contrast to the back flow in lee eddies in a steady unidirectional flow, which is usually only a fraction of the velocity in the main flow.

Another point is worth mentioning. The total excursion of the main water flow is often less than twice the ripple length.

Thus the flow pattern above the level of the ripple crests does not, as one might expect, attain the character of an oscillatory boundary layer in the known sense with the ripple height as a measure of the bed roughness. In fact the flow structure is entirely dominated by the regular eddies, their interaction and decay into turbulence.

Finally direct visual observations and high speed movies of the motion of the sand particles indicate that actual bed load transport as known from unidirectional flow hardly occurs. In fact one gets the impression that once a sand grain has started to move it goes into suspension (often via the eddy) before it settles again. This is also in disagreement with Longuet-Higgins (1972, p. 213) who (quoting Inman) claims that 'most of the weight of sediment is indeed in bed load, and not in suspended load.'

3. OUTLINE OF A THEORETICAL MODEL

We assume on the basis of these observations that *all* sediment is moved in suspension. The sediment is brought into suspension by a pick-up mechanism (as described above), which is further discussed in § 6. In the model it is described by the amount of solid sediment p(t) being picked up per unit area of bottom per second, and the mean value of p(t) over one period will be determined experimentally.

We further assume that the balance between the agitating processes tending to keep the sediment in suspension, and the settling of sediment (described by settling velocity w) has the nature of a diffusion process (irrespective the above mentioned regular nature of the eddy motion) with a diffusion coefficient ε, which is independent of time and horizontal coordinate x. (In fact the latter corresponds to averaging over a ripple length.) Thus the concentration c(z,t) of suspended sediment satisfies the diffusion equation

$$\frac{\partial c}{\partial t} - w\frac{\partial c}{\partial z} - \frac{\partial}{\partial z}\left(\varepsilon\frac{\partial c}{\partial z}\right) = 0 \tag{2}$$

z being the vertical coordinate.

The assumption of a pick-up mechanism p(t) implies that the process of bringing the sand into suspension is independent of the settling of the sediments. In the mathematical formulation this function acts as the source for the diffusion equation (2), thus representing the boundary condition at the bottom level z_b

$$-\varepsilon\frac{\partial c}{\partial z} = p(t) \qquad \text{at} \quad z = z_b \tag{3}$$

One advantage of this formulation is that it is considered easier to suggest physically realistic descriptions for the pick-up function p(t) (which could e.g. be proportional to the bottom shear stress) than for e.g. the bottom concentration c_b, often used as a boundary condition in suspension models.

As the second boundary condition in z is used $c(z) \to 0$ for $z \to \infty$ (though the water depth is h), and the system is closed in time by a periodicity assumption

$$c(z,t+T) = c(z,t) \tag{4}$$

When c(z,t) has been determined the instantaneous flux Q(t) of sediment through a vertical section is readily determined from the horizontal water velocity u(z,t) by

$$Q(t) = \int_0^h u(z,t)\ c(z,t)\ dz \tag{5}$$

and the net sediment flux then follows from

$$\overline{Q} = \frac{1}{T}\int_0^T Q\ db \tag{6}$$

At this point the model is more detailed than e.g. the approach used by Madsen and Grant (1976) who only consider the net motion of sediments. A closer inspection of the system shows that the clear separation of the pick-up and settling processes yields a memory effect in the model which implies that the maximum of sediment in motion occurs later than the maximum of p, and also that the sediment motion does not vanish with p, which may itself show a phase difference relative to the fluid motion. This is a generalization of the idea of a phase lag between shear stress and sediment motion introduced by Kennedy (1963), and used in waves by Kennedy and Falcon (1965). It will be shown that this effect is crucial for the understanding of the onshore-offshore transport.

4. GENERAL SOLUTION

In the general solution the pick-up function p(t) is considered in terms of its fourier series, which is assumed to have the form

$$\left.\begin{aligned} p(t) &= \sum_{0}^{N} P_n \cos n(\omega t - \psi_n) \\ p(t) &= \mathrm{Re}\left\{\sum_{0}^{N} P_n \, e^{in(\omega t - \psi_n)}\right\} \end{aligned}\right\} \quad (7)$$

The z coordinate is zero at the level of the ripple crests which is also chosen as the level for the boundary condition (3), i.e. $z_b = 0$.

The phase angle ψ_n in (7) accounts for the phase difference between p and the water motion which will be assumed to vary as $e^{in\omega t}$.

The equation is solved by separation of variables, and to facilitate the calculations the physical concentration is considered to be the real part of the complex function

$$c(z,t) = \sum_{0}^{N} C_n \, e^{in\omega t} \, \zeta_n(z) \quad (8)$$

where for simplicity we assume

$$\zeta_n(0) = 1 \quad (9)$$

Inserting (8) in the diffusion equation (2) leads to

$$\zeta_n'' + \left(\frac{w + \varepsilon'}{\varepsilon}\right) \zeta_n' - i \, \frac{n\,\omega}{\varepsilon} \, \zeta_n = 0 \quad (10)$$

where $\varepsilon' = d\varepsilon/dz$. The experiments presented later show that ε does not vary with z in non-breaking waves. If this is introduced into (10), an equation with constant coefficients results

$$\zeta_n'' + \frac{w}{\varepsilon} \zeta_n' - i \, \frac{n\,\omega}{\varepsilon} \, \zeta_n = 0 \quad (11)$$

which can be solved by standard methods.

Invoking (11) and the boundary condition $\zeta_n \underset{z\to\infty}{\to} 0$ we get

$$\zeta_n(z) = e^{-\frac{w}{\varepsilon}\cdot\alpha_n z} \quad (12)$$

where

$$\alpha_n = \frac{1}{2} + \sqrt{\frac{1}{4} + i\,\frac{n\,\omega\,\varepsilon}{w^2}} \quad (13)$$

The complex coefficients C_n in (8) are determined by the boundary condition (3), which using (8) becomes

$$-\,\varepsilon \, \frac{\partial}{\partial z}\left(C_n \, e^{in\omega t} \, \zeta_n\right) = P_n \, e^{in(\omega t - \psi_n)} \quad (14)$$

from which we get

$$c_n = \frac{P_n}{w\,\alpha_n}\,e^{-in\psi_n} \tag{15}$$

For n = 0 this yields a relation between the steady part of c(o,t) and the steady part of p(t)

$$c_o = \frac{P_o}{w} \tag{16}$$

which enables us to determine P_o from measurements of $C_o = \overline{c(o,t)}$, where the bar denotes mean value over a wave period.

Thus the complete solution for the concentration profile as a function of time becomes

$$\left.\begin{aligned} c(z,t) &= \sum_{0}^{\infty} \frac{P_n}{w\,\alpha_n}\, e^{in(\omega t-\psi_n)}\; e^{-\frac{w}{\varepsilon}\alpha_n z} \\ \alpha_n &= \frac{1}{2} + \sqrt{\frac{1}{4} + i\,\frac{n\,\omega\,\varepsilon}{w^2}} \end{aligned}\right\} \tag{17}$$

We note that $\varepsilon\omega/w^2$ is an important parameter, which represents the ratio of the response time for the concentration profile ε/w^2 over the wave time scale $T/2\pi$. This information could, of course, also be extracted directly from (2) by non-dimensionalization.

The physical concentration is obtained as the real part of (17), which is

$$c(z,t) = \sum_{0}^{\infty} \frac{P_n}{w\,|\alpha_n|}\,\cos n\left[\omega t - \psi_n - \frac{1}{n}\left(\arg\,\alpha_n + \frac{w\,z}{\varepsilon}\,\mathrm{Im}\{\alpha_n\}\right)\right] e^{-\frac{wz}{\varepsilon}\mathrm{Re}\{\alpha_n\}} \tag{18}$$

Fig. 2 shows the variation of α_n, and Fig. 3 that of $|\alpha_n|$, arg α_n, Re $\{\alpha_n\}$, and Im $\{\alpha_n\}$.

Finally the sediment flux Q is determined from (5). Here we assume that the ripple length λ is small, i.e. $\lambda \ll L$, where L is the wave

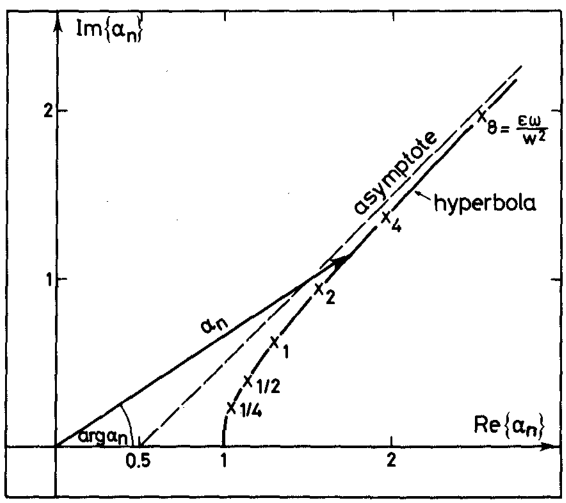

Fig 2
The position of α_n in the complex plane.

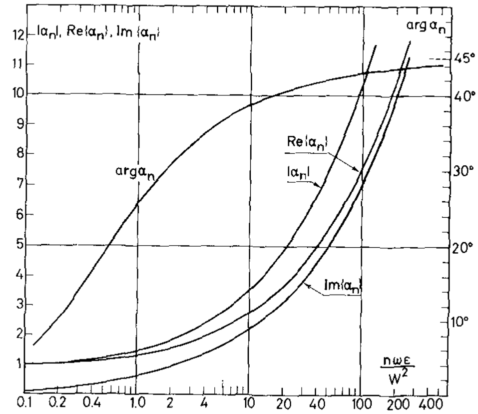

Fig. 3
The magnitude of $|\alpha_n|$, $Re\{\alpha_n\}$, $Im\{\alpha_n\}$ and $\arg \alpha_n$ versus $n\omega\,\varepsilon/W^2$.

length, so that the horizontal water velocity is approximately constant over λ, and the averaging over a ripple length introduced earlier can be executed with a constant $u(z,t)$. Thus for convenience we assume that u has the form

$$u(z,t) = \sum_{0}^{N} u_n(z) \cos n\,\omega t \tag{19}$$

which include a term $u_o(z)$ constant in time. Substituting this and (8) into (6) yields

$$\overline{Q} = \frac{1}{T} \int_0^T \int_0^T \sum_{0}^{N} c_n(z,t)\; u_n(z,t)\; dz\; dt \tag{20}$$

which is a general expression for Q. To get practical results from this expression we must specify the value of the diffusion coefficient ε, a problem which is discussed in § 5. We must also know the form of the pick-up function p (i.e. the fourier-coefficients P_n in (7) and the phase angle ψ_n). This is discussed in § 6. And finally $u_n(z)$ is required. However, the formulation above is actually too general for detailed discussion, and a number of useful conclusions can be obtained from studying special examples. This will be discussed in § 7.

5. PREDICTION OF THE DIFFUSIVITY

One of the basic assumptions behind this model is that the upward flux of sediment at any level is due to diffusion as expressed by the term $- \varepsilon\, \partial c/\partial z$.

To test this assumption and to obtain results for ε, the sediment concentrations were measured over a sand bed subjected to waves in a 60 cm wide wave flume with a water depth of about 40 cm. The water/sand mixture was sucked out through thin pipes (1,5 mm diameter) at different levels, and the concentration determined from the sample. Thus all measurements represented mean values over several wave periods. In addition to these results, measurements published by Nakato et al. (1977), and some unpublished results performed in the pulsating water tunnel described by Lundgren and Sørensen (1958), have been used in the following analysis.

The value of ε for each experiment was determined graphically from a semilogarithmic plot of the measured concentrations versus the vertical coordinate z. Fig. 5 shows examples of such plots which clearly illustrate that ε is nearly constant under non-breaking waves, and also may be taken as a support of the assumption that the phenomenon may be approximated by a diffusion process with ε = constant.

The results thus obtained for ε have been analysed in several ways. First it is worth to notice that Svendsen et al. (1977) analysed the motion of suspended particles in accelerated flow and found that sand grains would follow the oscillatory water motion practically identically (apart from the settling due to gravity). From their results for sinusoidal oscillations may be deduced that even in the relatively low frequency turbulence in the flow in question, the grains must very nearly follow the water flow, from which we can conclude that the diffusivity ε is equal to the turbulent eddy viscosity ν_T.

ε or ν_T are often considered as the product of a typical length scale l_ε and a typical velocity u_ε.

A natural length scale (of vertical motion) in the flow over a ripple bed is the ripple height η.

When no ripples are present, the scale is $\kappa\,\delta$, where κ is Von Karman's constant and δ the boundary layer thickness. δ may then be calculated from the equation

$$\delta/a = 0.072\ (2.5\,d/a)^{0.25} \tag{21}$$

as given by Jonsson and Carlsen (1976).

For the characteristic velocity u_ε, is normally used the friction velocity $u_f = \sqrt{\tau_{max}/\rho}$. One might then conjecture a simple relation like

$$\varepsilon = F(u_f[\eta + \kappa\ \delta]) \tag{22}$$

where $\kappa\ \delta \ll \eta$ in situations with noticeable ripples.

In fact it turns out that the best empirical correlation in the results for ε is obtained if we use

$$\frac{\varepsilon}{(\eta + \kappa\ \delta)\ g\ T} = f\left(\frac{U_m}{w}\right) \tag{23}$$

as shown in Fig. 4. The physical background, however, of this correlation is not clear, and the subject obviously needs further consideration.

The diffusivities mentioned above are all determined in non-breaking waves and from measurements of concentrations within about 5 ripple heights from ripple crest level. Above this level there is hardly any bed material in suspension.

If, however, the waves are just gently breaking as spilling breakers, the turbulence generated by the breaking will reach the bottom after 4 - 6 wave periods, and significantly change the shape of the concentration profile, down to a few ripple heights (centimeters) above the bed. As a result the suspended material is spread from surface to bottom. The effect is surprisingly strong, particularly for fine materials with large u/w, and indisputable as shown in Fig. 5, where the concentration profile from under a spilling breaker is shown together with that of an unbroken wave with the same height. It also forms a remark-

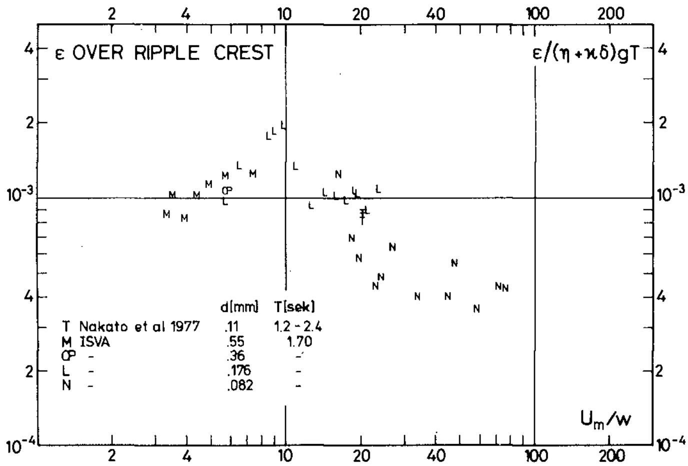

Fig. 4 A plot for semi-empirical determination of ε from U_1/w and the vertical length scale $(\eta + \kappa\delta)$.

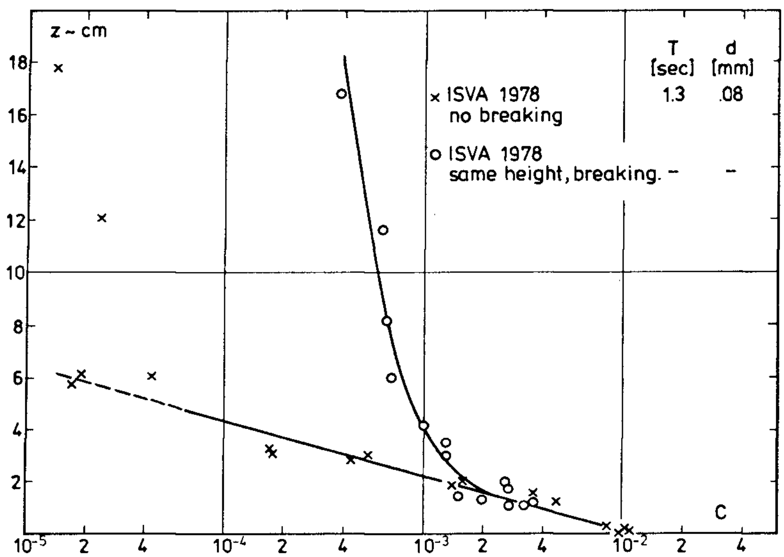

Fig. 5 The distributions of suspended sediment under breaking and non-breaking waves of equal heights. Breaking gives much larger diffusivities but slightly smaller concentrations at the bed level.

able illustration to the ideas about the turbulence conditions in spilling breakers presented by Peregrine and Svendsen (1978).

It should be noticed that the concentrations at the bed level are nearly unchanged by the breaking, and the measurements show that the total amount of sediment in suspension is practically unchanged too. This indicate that the pick-up process is only moderately affected by the surface turbulence, which has been decaying over 4 - 6 wave periods before it reaches the bottom. On the other hand, the relative change in turbulent intensity is large from the surface down to about 5 times the ripple height above the bed, and the already suspended sand is easily spread over a whole depth of water.

6. ANALYSIS OF PICK-UP FUNCTION

The pick-up function p(t) is always non-negative and therefore has a positive time mean value P_o. In the following we divide the discussion between P_o, which is determined experimentally, and the time variation of p(t) (i.e. the rest of fourier-coefficients in (7)).

The time mean value of p(t)

In the solution for c(z,t) we found in § 4 that the true mean value P_o of p(t) was equal to $w\,C_o$ where C_o in the time mean value of the concentration at z = 0. This means that P_o can be determined directly from the measurements described in the previous paragraph.

A closer analysis af these shows that C_o depends on the horizontal position of the measuring point relative to the ripple. C_o is larger over the crest than over the trough. We find that $C_{o,crest} \approx 1.8 \cdot C_{o,trough}$.

However, the net transport $\overline{Q}$ must be the same through any vertical section. And since we have chosen our reference level z = 0 at the level of the ripple crest to be consistent, we must also in the calculations use the C_o values obtained over the ripple crest.

Fig. 6 shows the measured values of $C_{o,crest}$ as a function of the Shields' parameter θ' (i.e. the non-dimensional shear stress) given by (1), in which we have used Swart's (1974) empirical fit to the experimental results for f_w in an oscillatory boundary layer, i.e.

$$f_w = \exp\{5.213\ (2.5\,d/a)^{0.195} - 5.977\} \tag{24}$$

It is important here that f_w is based on grain-roughness, not on the ripple-height, say.

As we see from the figure, the results for C_o varies fairly consistently with θ'.

The time variation of p(t)

As mentioned in § 2 most of the sediment grains that move over a rippled bed are ripped off the upstream side of the ripples, pass over the crest into the lee eddy, and are then washed out into real suspension with that eddy. Thus we must expect the pick-up function p(t) to show significant peaks twice every wave period. No measurements are available to quantify this, but observations in a wave flume or on a beach clearly show strong puffs with high concentration of sediments

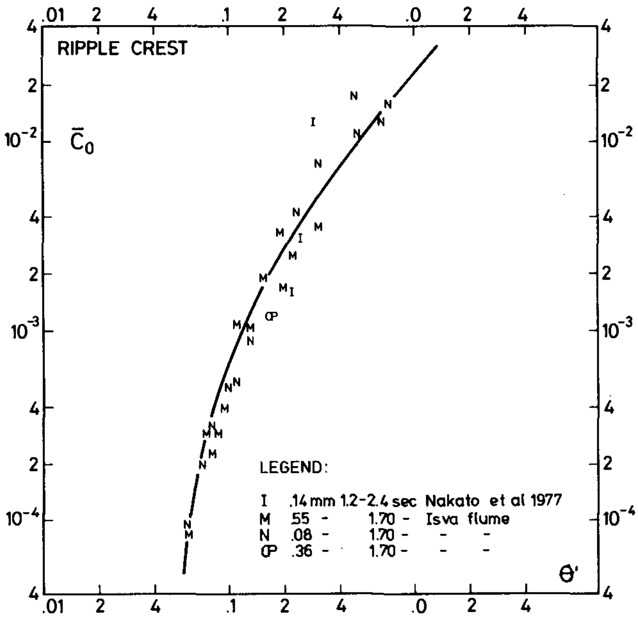

Fig. 6 The steady part of the concentration at ripple crest level is a function of θ'.

emerging in the general 'pea soup' over each ripple, and at the right time. Often the puffs occurring right after the wave crest has passed (i.e. after the highest velocities) are more significant than those produced after the weaker return flow in the wave trough.

Tentatively this can be modelled by a pick-up function of the form

$$p(t) = \frac{P_o}{1+\beta}\,\frac{(2m)!!}{(2m-1)!!}\left\{\cos^{2m}\frac{1}{2}(\omega t - \psi^+) + \beta\,\cos^{2m}\frac{1}{2}(\omega t - \psi^-)\right\} \qquad (25)$$

where m is a positive integer,* and β is accounting for the difference between crest and trough velocities. β may be determined as

$$\beta = \left(\frac{u_{trough}}{u_{crest}}\right)^2 \qquad (26)$$

with the u's as maximum values of the bottom velocities in the water motion (notice that weak currents may be included here).

According to the description above the phase angles ψ^+ and ψ^- are determined as the phases where the velocity in the main flow is changing direction. Notice that this choice, however surprising, may also be expected to apply as an approximation to the case of a plane bed. Then the thin boundary layer adhering to the bottom separates shortly before the time of velocity shift, yielding a situation similar (though less pronounced) to the release of eddies over the ripple bed.

$*\,(2m)!! = 2\cdot 4\cdot \ldots\cdot 2m;\quad (2m-1)!! = 1\cdot 3\cdot 5\cdot \ldots\cdot (2m-1).$

Thus ψ^+ and ψ^- depend on the wave motion considered. In the examples in the following paragraph $\psi^+ = \psi^- - \pi = \pi/2$ for sinusoidal waves (example (1)), whereas $\psi^+ < \pi/2$ and $\psi^- > 3\pi/2$ for second order Stokes waves with zero mass flux (example (2)).

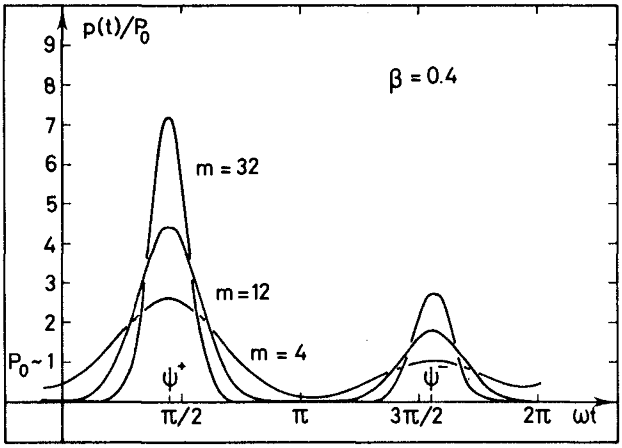

Fig. 7 The time-variation of the pick-up function for different values of the power 2m.

The exponent 2m gives the shape of the pick-up function. For $m \to \infty$ (25) corresponds to two δ-functions at $\omega t = \psi^+$ and ψ^-, respectively. Fig. 7 shows some examples for different choices of m. The important point, however, how much the choice for m is influencing the results for $\overline{Q}$ is analysed in more details in example (2).

7. EXAMPLES

(1) Sinusoidal wave motion

The simplest example one can think of is that of a sinusoidal wave, where

$$u(t) = U_1 \cos \omega t \tag{27}$$

Here p(t) must have two peaks, equal in height and with a phase difference of π, i.e. $\beta = 1$ in (25), so that p(t) is

$$p(t) = P \cos^{2m}(\omega t - \psi) \tag{28}$$

Without loss of generality we can take m = 1 to obtain

$$p(t) = P_o(1 + \cos 2(\omega t - \psi)) \tag{29}$$

Fig. 8 shows the variation of the pick-up function and the concentration at the bed level in this case.

We see from (15) that the phase shift is $\frac{1}{2}$ arg α_2, and that c(o,t) does not go to zero as p(t) does. Hence this important property of the suspension mechanism is modelled correctly because of the separation between the pick-up and settling process.

Equation (20) shows that $\overline{Q} = 0$ because of the symmetry of the problem. Note that this result is independent of ψ and of the power 2m in (28).

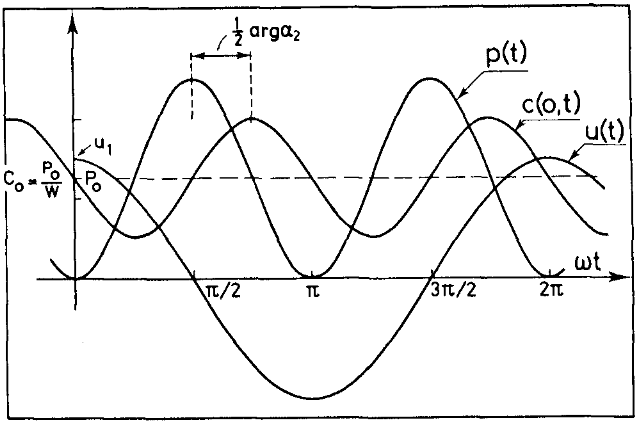

Fig. 8 The variation mode of p(t) and c(o,t) when u(t) is simple harmonic. Note that c(o,t) is not in phase with p(t), and that c(o,t) does not go to zero as p(t) does.

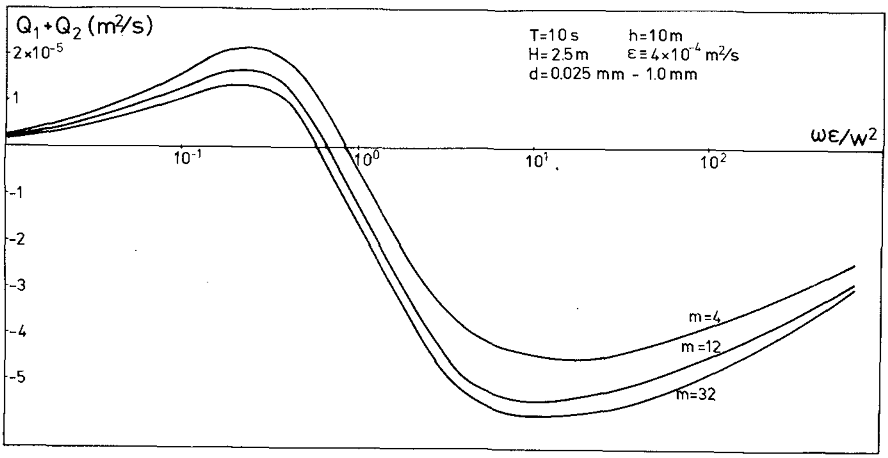

Fig. 9 The choice of m is not critical for $Q_1 + Q_2$. (Q_o is independent of m).

(2) Second order Stokes' wave

In the second example we assume a second order Stokes' wave motion, i.e. a velocity u at the bottom given by

$$\left.\begin{aligned} & u = U_o + U_1 \cos\omega t + U_2 \cos 2\omega t \\ & \text{with} \\ & U_1 = \frac{\pi H}{T \sinh kh} \qquad U_2 = \frac{3}{16}\, c\, \frac{(kH)^2}{\sinh^4 kh} \end{aligned}\right\} \quad (30)$$

i.e. we neglect the z-variation of u. Notice that U_o can represent a 'return flow' corresponding to a zero net mass transport (i.e. (30) will represent a pure wave motion), if

$$U_o = -\frac{1}{8}\frac{gH^2}{ch} \quad (31)$$

If (30) is substituted into (20) together with (25), we get the following expression for the net sediment flux

$$\overline{Q} = \frac{U_o P_o \varepsilon}{2w^2(1+\beta)}\left\{2(1+\beta) - \sum_{n=1.2} \frac{a_n U_n}{U_o |\alpha_n|^2}\left\{\cos(n\psi^+ + 2\arg\alpha_n) + \beta\cos(n\psi^- + 2\arg\alpha_n)\right\}\right\}$$

$$\equiv Q_o + Q_1 + Q_2 \quad (32)$$

The parameters of this expression are the wave data H/L and $T\sqrt{g/h}$, the grain diameter d, and m. Fig. 9 shows for a particular wave the influence on the oscillatory part of $\overline{Q}$ (i.e. $Q_1 + Q_2$) of three choices for m in the range, which is considered realistic. $m \to \infty$ yields less than 10% change in $\overline{Q}$ relatively to m = 32. The dependence on m is moderate, and we choose m = 12 in the following.

The results for the ripple height η required for evaluation of ε from Fig. 7 have been obtained from the mean curve shown in Fig. 10, which gives η/a (a being the water particle amplitude at the bottom determined from linear theory) versus $U_1^2/(s-1)gd$, s being the relative density of the sand.

Figs. 11 through 14 show the variation of $Q_1 + Q_2$, Q_o and the net discharge $\overline{Q}$ for waves with $T\sqrt{gh} \cong 10$ and height up to 4 metres (0.4 times depth of water), and four typical grain diameters d = 0.1, 0.2, 0.4 and 1 mm. In these calculations U_o has been determined from (31), i.e. the $\overline{Q}$ represents zero net transport in the water motion. Some characteristic values of ε and θ' obtained in the computations are shown in the figures too.

The figures show that under these conditions the sediment will move seawards under almost all wave conditions ($\overline{Q} < 0$).

A number of other observations and conclusions may be extracted from the results.

(i) The rather sharp decrease in the numerical value of all Q-curves corresponds to the region between $\theta = 0.4$ and $\theta = 1.0$, where the ripples suddenly disappear and ε, as given by Fig. 4 and Fig. 10, consequently decreases by a factor of 10.

(ii) For the larger grains sizes the oscillatory contributions are positive (shoreward movement) for high waves, and of the same order of magnitude as Q_o. Thus if Q_o had been less negative (or even positive) —

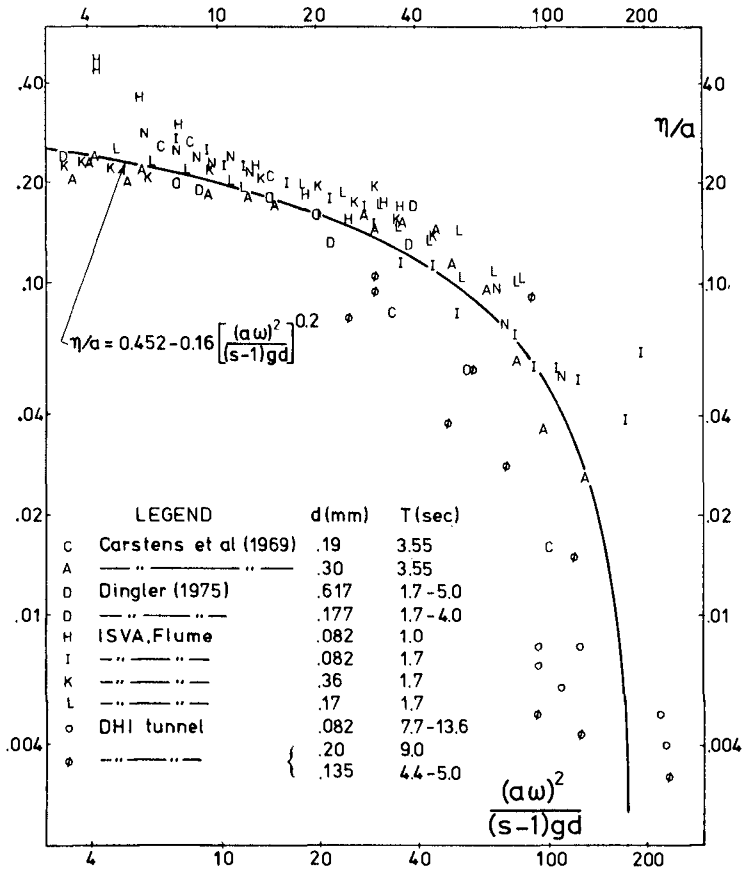

Fig. 10 Semi-empirical plot for determination of the ripple height η

for instance due to three-dimensional effects, vide the introduction — $\overline{Q}$ might well have been positive.

(iii) The finer the material, the less important the oscillatory part, and for d = 0.1 mm net sediment discharge is entirely dominated by Q_o, i.e. U_o. Then the net sediment flux may be determined by

$$\overline{Q} \approx Q_o = U_o\, P_o\, \varepsilon/w^2 \tag{33}$$

and this corresponds to situations where the variation of c over a wave period is small.

(iv) The values obtained for ε by the procedure described above appear in a wide region without ripples to be close to $1/4\,\kappa\, U_f \delta$ (κ von Karman's constant, U_f friction velocity, δ boundary layer thickness). This estimate can in fact be inferred from Kajiura (1968) (Jonsson, private communication). Since part of this region is outside the region where measurements for ε are available, this is taken as an indication that our extrapolations in the computations are reasonable.

Finally it is emphasized that all these results apply to non-breaking waves only.

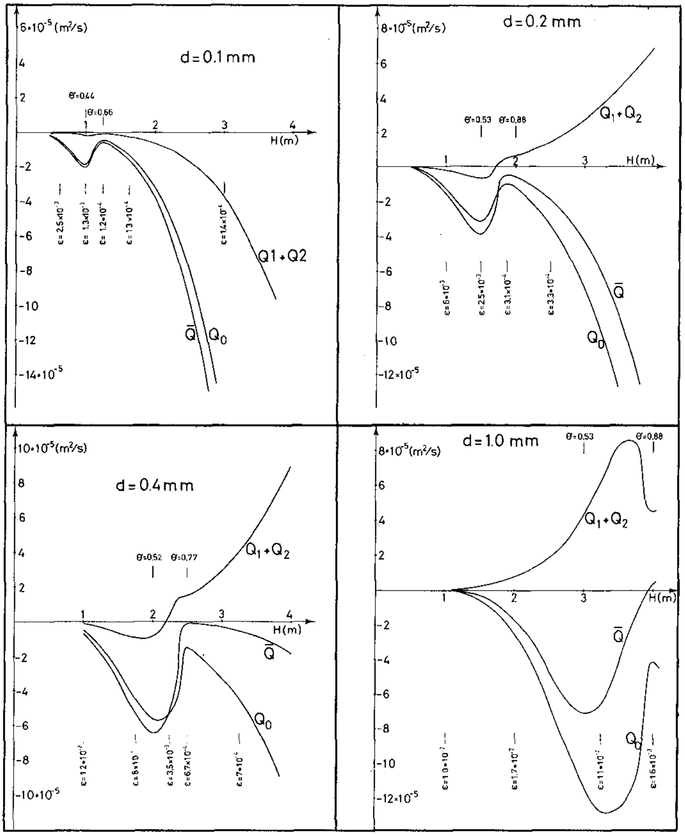

Fig. 11 - 14 Transport versus wave height for different grain diameters. ($U_o = - gH^2/8ch$).

Comparison with experiments

The model has also been compared with measurements in a wave flume. Fig. 15 shows measurements of $\overline{Q}$ obtained on a horizontal bottom from the changes in bed elevation over a recorded number of waves. Fig. 16 shows the corresponding measurements of the mean water velocity U_o. When this is used in the calculation of $\overline{Q}$, we get the value shown by the dotted line in Fig. 15. (The straight line approximation in Fig. 16 was used for U_o).

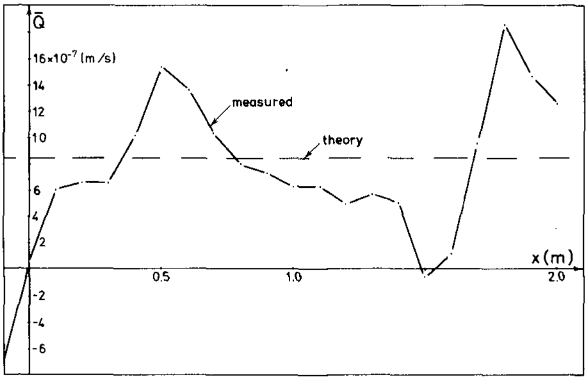

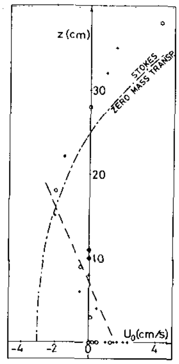

Fig. 15 - 16 Calculated and measured transport for a flume experiment. (ISVA, 1978).

8. CONCLUSIONS

A theoretical model has been developed which yields analytical results for the instantaneous distribution of sediment concentrations $c(z,t)$, when the oscillatory water motion (the wave) and the net mass flux (the current) is prescribed. The result for c is given by (17). Also the sediment flux (instantaneous and time mean) is determined (Eqs. 5 and 6).

Experiments are used to determine the diffusion coefficient ε (§ 5) required as input to the model (Fig. 4), and the results indicate that it is reasonable as done to assume the suspension of sediment can be approximated by a diffusion process. The actual physics of the sediment motion is described and discussed in detail in § 2.

In the solution a pick-up function $p(t)$ occurs. Mathematically it acts as the boundary condition at the sea bed for the diffusion equation (§ 3 - 4). Physically it accounts for the process (also described in § 2) of picking up the sand and bringing it into suspension. The mean value of $p(t)$ is determined experimentally in § 6 where also the time variation of this process is discussed, and equation (25) is a heuristic suggestion for $p(t)$ and further discussed in example (2) in § 7.

In § 7 two examples are analysed, showing the consequences of the model for the onshore-offshore sediment flux in two different wave motions. The first (a simple sinusoidal wave) always yields zero net sediment movement.

In the second example a second order Stokes' wave with specified mass flux is considered. Here the results are far more complicated. For a wave motion with zero net mass flux, the net sediment motion $\bar{Q}$ is always against the wave direction. The balance, however, is delicate, and in a pure oscillatory flow (no return flow) the motion may go in either direction (Figs. 11 through 14).

Finally the model is compared with a measurement of $\overline{Q}$ in a wave flume with zero net water flux, using a second order Stokes' wave model and a measured mean water velocity profile (Fig. 16). In Fig. 15 the computed and measured values of $\overline{Q}$ are shown to compare within the accuracy of the measurements.

References

Allen, J.R.L. (1968) Current Ripples. North-Holland Publ. Co., Amsterdam.

Bijker, E.W., E. van Hijum and P. Vellinga (1976) Sand transport by waves. Proc. 15th Coastal Engrg. Conf., Hawaii, pp. 1149-1167.

Dingler, J.R. (1974) Wave Formed Ripples in Nearshore Sands. Ph.D. thesis, Univ. Calif., San Diego, 136 pp.

Fredsøe, J. (1978) Natural backfilling of pipeline trenches. Proc. 10th Offshore Tech. Conf., Houston, Texas, OTC 3073, pp. 225-232.

Inman, D.L. (1957) Wave generated ripples in nearshore sands. Tech. Memo 100, Beach Erosion Board, 55 pp.

Jonsson, I.G. and N.A. Carlsen (1976) Experimental and theoretical investigations in an oscillatory turbulent boundary layer. J. Hydr. Res., Vol. 14, No. 1, pp. 45-60

Kajiura, K. (1968) A model of the bottom boundary layer in water waves. Bull. Earthquake Res. Inst., Univ. Tokyo, Vol. 46, Ch. 5, pp. 75-123.

Kennedy, J.F. (1963) The mechanics of dunes and antidunes in erodible-bed channels. J. Fluid Mech., Vol. 16, No. 4, pp. 521-544.

Kennedy, J.F. and M. Falcon (1965) Wave generated sediment ripples. M I T, Hydrodyn. Lab., Rep. No. 86, 55 pp.

Longuet-Higgins, M.S. (1972) Recent progress in the study of longshore currents. In: Waves on Beaches and Resulting Sediment Transport, Proc. Adv. Sem., Madison, Wisconsin. Ed. R.E. Meyer. Academic Press, pp. 203-248

Lundgren, H. and T. Sørensen (1958) A pulsating water tunnel. Proc. 6th Coastal Engrg. Conf., Florida, pp. 356-358.

Madsen, O.S. and W.D. Grant (1976) Sediment transport in the coastal environment. M I T, Ralph M. Parsons Lab. Water Res. Hydrodyn., Rep. No. 209, 120 pp.

Nakato, T., F.A. Locher, J.R. Glover and J.F. Kennedy (1977) Wave entrainment of sediment from rippled beds. A S C E, Vol. 103, WW1, pp. 83-100.

Nielsen, P. (1977) A note on wave ripple geometry. ISVA, Tech. Univ. Denmark, Prog. Rep. 43, pp. 17-22.

Peregrine, D.H. and I.A. Svendsen (1978) Spilling breakers, bores and hydraulic jumps. Proc. 16th Coastal Engrg. Conf., Hamburg.

Svendsen, I.A., P. Nielsen and C. Staub (1977) The motion of suspended particles in oscillatory flow. ISVA, Tech. Univ. Denmark, Prog. Rep. 44, pp. 13-18

Swart, D.H. (1974) Offshore sediment transport and equilibrium beach profiles. Delft Hydr. Lab., Publ. No. 131.

Tunsdall, E.B. and D.L. Inman (1975) Vortex generation by oscillatory flow over rippled surfaces. J. Geophys. Res., Vol. 80, No. 24, pp. 3475-3485.